INSTITUTE OF PHYSICS PUBLISHING CLASSICAL AND QUANTUM GRAVITY

Class. Quantum Grav. **18** (2001) 2015–2024 www.iop.org/Journals/cq PII: S0264-9381(01)22832-9

An axially symmetric scalar field as a gravitational lens

Tonatiuh Matos[1] **and Ricardo Becerril**[2]

[1] Depto de Física, CINVESTAV IPN, AP 14-740, 07000 México DF, Mexico
[2] Instituto de Fisica y Matemáticas, Universidad Michoacana, AP 2-82, 58040, Morelia, Mich., Mexico

Received 15 March 2001

Abstract

The gravitational lensing due to an axially symmetric lens with a minimally coupled scalar field is considered. Comparison is made with the case of a spherically symmetric lens analysed previously in the literature, and a different dependence of the image positions on the 'scalar charge' is found. In particular, while the formation of four images, two Einstein rings and one radial critical curve (RCC) is possible for different configurations with both types of lenses, their positions are different from one metric to the other. Nevertheless, these differences are very small and, even if such configurations are ever observed, it seems to be very difficult to distinguish between the spacetimes studied here.

PACS number: 0420

1. Introduction

Although the deflection of light by the Sun was one of the first observations supporting general relativity (GR), the set of phenomena involving light deflection in a gravitational field (collectively referred to as gravitational lensing or GL for short) were considered as mere theoretical curiosities for a long time. However, the discovery of the first gravitationally lensed quasar in the late 1970s gave rise to an ever increasing interest both in the theoretical framework and in the observational identification of gravitational lenses in the Universe. Nowadays, GL has become a standard astronomical as well as cosmological tool, allowing for accurate measurements of parameters such as galaxies and galaxy clusters masses, quasar distances and the Hubble constant. Moreover, the spectrum of observations already includes configurations once thought exotic, such as actual Einstein rings or giant arcs.

On the other hand, there exist several alternatives or extensions to standard GR which include in their formulation one or more scalar fields, and they are collectively known as scalar–tensor (ST) theories of gravity. The scalar field, both minimally and conformally coupled to gravity has been the subject of intensive research in recent years, and in particular the dilaton has generated growing interest because of its importance in string theory. Although these matters could seem to be of little astrophysical relevance, phenomena such as 'spontaneous scalarization' in neutron stars [1] give some hope of actually observing scenarios where one or more scalar fields produce macroscopic effects. In different contexts, the scalar field has

0264-9381/01/112015+10$30.00

also been proposed as a candidate for gravitational lensing [2] and for the dark matter at galactic scales, where it may account for the flat rotation curves (see, e.g., [3]), as well as at cosmological scales [4, 5].

Along this line, GL can be a very powerful tool in testing these alternative theories in an astrophysical setting. One of the first proposals in this direction was the case of the hypothetical remnants of spontaneous symmetry breaking in the very early Universe, such as monopoles, cosmic strings, domain walls and others (see, e.g., [6]). Recent work by Virbhadra *et al* [2] has focused in the consequences of a spherical lens possessing a scalar field minimally coupled to gravity, making use of the Janis–Newman–Winicour [9] metric to model the spacetime surrounding such an object. Here we shall consider an axially symmetric field as a variation of this idea.

Our aim here is to present an analysis similar to that of Virbhadra *et al* [2], but now considering an axially symmetric solution to the field equations for gravity minimally coupled to a scalar field. To this end, we shall employ a Schwarzschild-like solution, which has been studied previously as part of the proposal that the magnetic field of astrophysical objects (such as neutron stars) could have its origin in the compactification processes of higher-dimensional field theories when a strong gravitational field is present [10].

The paper is organized as follows. In section 2 the solution to the field equations is introduced and some interesting features of it are mentioned; section 3 then presents the expression for the deflection angle at large distances from the source, and the main results for this weak lensing scenario (as well as some differences with the work by Virbhadra *et al* [2]) are shown in section 4; finally, section 5 presents some concluding remarks.

2. The action for the theory and the metric

The metric we shall use to describe the spacetime acting as a lens is an axially symmetric solution to the field equations derived from the action for gravity minimally coupled to a scalar field (here and throughout, units in which $c = G = 1$ are used):

$$S = \int \mathrm{d}^4x \, \sqrt{-g}(-R + 2\nabla^\mu \Phi \nabla_\mu \Phi) \tag{1}$$

where Φ is the scalar field. It should be noted that previously known solutions to the field equations are either spherically symmetric or too cumbersome to deal with. From the above action, the following field equations are obtained after variations with respect to the metric $g_{\mu\nu}$ and the scalar field Φ:

$$\begin{aligned} &\Phi^{;\mu}{}_{;\mu} = 0, \\ &R_{\mu\nu} = 2\Phi_{,\mu}\Phi_{,\nu}. \end{aligned} \tag{2}$$

On the other hand, it can be shown [11] that it is possible to find axially symmetric solutions which are rather simple. In fact, the metric we shall study was actually obtained in Matos *et al* [11] as a solution to dilatonic gravity, which is a theory originally derived from superstring-inspired models and features an exponential coupling between the scalar and any matter fields; for instance, for an electromagnetic field $F_{\mu\nu}$, an additional term $\mathrm{e}^{-2\alpha\Phi}F^{\mu\nu}F_{\mu\nu}$ should appear in the action, with α being a coupling constant. However, the equivalence principle tests put a very stringent bound on α, namely $\alpha < 10^{-12}$, while for string theory $\alpha = 1$. This implies that the full dilatonic theory is not well suited to model the gravitational interaction between macroscopic bodies. Therefore, we shall drop the dilatonic coupling (which does not eliminate the scalar field in the solutions found

in [11]) and concentrate on the above, simpler theory. We believe that it is worth trying to use these solutions to model the exterior field of macroscopic bodies, in order to look for any possible difference in their predictions with those of GR or other scalar–tensor theories.

The solution we shall consider is then

$$\mathrm{d}s^2 = -\left(1-\frac{2m}{r}\right)\mathrm{d}t^2 + \mathrm{e}^{2k_s}\frac{\mathrm{d}r^2}{1-2m/r} + r^2(\mathrm{e}^{2k_s}\,\mathrm{d}\theta^2 + \sin^2\theta\,\mathrm{d}\varphi^2), \tag{3}$$

with

$$\mathrm{e}^{2k_s} = \left(1+\frac{m^2\sin^2\theta}{r^2(1-2m/r)}\right)^{-1/a^2},$$

$$\Phi = \frac{1}{2a}\ln\left(1-\frac{2m}{r}\right),$$

where a is a constant of integration. It can be observed that, in the limit when $a \to \infty$, we recover the Schwarzschild solution, as can also be noted if we calculate the scalar charge for this metric; following [18] we obtain

$$Q_s = \frac{1}{4\pi}\oint_S \mathrm{d}^2 S^\mu \nabla_\mu \Phi = \frac{m}{a}, \tag{4}$$

where the integration is over a 2-sphere of radius R and the limit is taken when $R \to \infty$ (Q_s can also be simply read off from the $1/r$ term in the expansion of Φ in powers of $1/r$); in this case, when $a \to \infty$ we have $Q_s \to 0$, corresponding to GR.

Let us finally note that this solution does not describe a spacetime with rotation, which is what usually breaks the spherical symmetry; instead, its axial character arises from the presence of the scalar field, even though this field is spherically symmetric. While axially symmetric solutions with spherical sources are known in GR (see, e.g., [12]), the description of suitable sources with a scalar field is not straightforward; therefore, and because of its similarity with the Schwarzschild solution, we shall assume that the above metric can be employed to model the exterior field of a macroscopic object endowed with a minimally coupled scalar field, and that it can be matched to a regular interior solution. The analysis of this interior problem is currently being carried out numerically [13].

3. Deflection angle and image formation

Let us now turn to the deflection of light when it travels in the spacetime defined by the metric (3). To this end, we must write down the equation governing the null geodesics; following standard methods [14, 15], one is led, from the Lagrangian for photons:

$$\mathcal{L}_{ph} = -\left(1-\frac{2m}{r}\right)\left(\frac{\mathrm{d}t}{\mathrm{d}s}\right)^2 + \frac{\mathrm{e}^{2k_s}}{1-2m/r}\left(\frac{\mathrm{d}r}{\mathrm{d}s}\right)^2 + r^2\left(\mathrm{e}^{2k_s}\left(\frac{\mathrm{d}\theta}{\mathrm{d}s}\right)^2 + \sin^2\theta\left(\frac{\mathrm{d}\phi}{\mathrm{d}s}\right)^2\right) = 0,$$

(s is the affine parameter) to the path equation for photons:

$$\left(\frac{\mathrm{d}r}{\mathrm{d}s}\right)^2 + \mathrm{e}^{-2k_s}\left(\frac{B^2}{r^2}\right)\left(1-\frac{2m}{r}\right) = \mathrm{e}^{-2k_s}A^2 \tag{5}$$

where we have set $\theta = \pi/2$ for simplicity (i.e. we consider only equatorial trajectories), and A and B are the constants of motion corresponding to t and φ, respectively:

$$A = \left(1 - \frac{2m}{r}\right)\frac{\mathrm{d}t}{\mathrm{d}s},$$

$$B = r^2\frac{\mathrm{d}\varphi}{\mathrm{d}s}.$$

Next, noting that $\mathrm{d}r/\mathrm{d}s = (\mathrm{d}r/\mathrm{d}\varphi)(\mathrm{d}\varphi/\mathrm{d}s)$, and using the fact that, at the minimum distance r_0 to the lens, $\mathrm{d}r/\mathrm{d}\varphi = 0$, we obtain, as usual,

$$B = \frac{Ar_0}{\sqrt{1-2m/r_0}}. \tag{6}$$

Substituting back in the geodesic equation (5), the following expression can be derived:

$$\varphi(r_2) - \varphi(r_1) = \int_{r_1}^{r_2}\frac{\mathrm{d}r}{r}\left(\frac{(1-m/r)^2}{1-2m/r}\right)^{-1/2a^2}\left[\frac{r^2}{r_0^2}\left(1-\frac{2m}{r_0}\right) - \left(1-\frac{2m}{r}\right)\right]^{-1/2}. \tag{7}$$

Denoting by $\hat{\alpha}(r_0)$ the total deflected angle and performing a series expansion in powers of m/r_0 (weak-field limit) we obtain, up to order m^2/r_0^2,

$$\begin{aligned}\hat{\alpha}(r_0) &= 2|\varphi(r) - \varphi(\infty)|_{r=r_0} - \pi \\ &= \frac{4m}{r_0} + \frac{m^2}{r_0^2}\left(\frac{15\pi}{4} - 4 - \frac{\pi}{4a^2}\right) + \mathcal{O}\left(\frac{m^3}{r_0^3}\right),\end{aligned}$$

which can be easily cast in terms of the ratio of the scalar charge to the mass, $R_{sm} \equiv Q_s/m = 1/a$:

$$\hat{\alpha}(r_0) = \frac{4m}{r_0} + \frac{m^2}{r_0^2}\left(\frac{15\pi}{4} - 4 - \frac{1}{4}\pi R_{sm}^2\right) + \mathcal{O}\left(\frac{m^3}{r_0^3}\right). \tag{8}$$

Since metric (3) is very similar to the Schwarzschild spacetime, we can expect its expansion in powers of m/r_0 to be very similar to the Schwarzschild case, and indeed both coincide up to order $\mathcal{O}(m/r)$. However, the next terms in the expansion depend on the scalar charge Q_s, and if we put $Q_s = 0$ we recover the expression for the Schwarzschild solution, as we should. A similar behaviour was found for a spherical scalar field by Virbhadra *et al* [2]; using the well known Wyman solution [7], which is also a solution to the field equations (2). Virbhadra also showed that Wyman and Janis–Newman–Winicour solutions are just the same [8], but JNW had found their metric much before Wyman. Their metric reads [9],

$$\begin{aligned}\mathrm{d}s^2_{JNW} &= -\left(1-\frac{b}{r}\right)^{\gamma}\mathrm{d}t^2 + \left(1-\frac{b}{r}\right)^{-\gamma}\mathrm{d}r^2 - \left(1-\frac{b}{r}\right)^{1-\gamma}r^2(\mathrm{d}\theta^2 + \sin^2\theta\,\mathrm{d}\phi^2), \\ \Phi &= \frac{q}{b}\ln\left(1-\frac{b}{r}\right),\end{aligned} \tag{9}$$

where

$$\gamma = \frac{2m}{b}, \qquad b = 2\sqrt{m^2+q^2},$$

and q is again the scalar charge, they found the following expression:

$$\hat{\alpha}_{JNW}(r_0) = \frac{4m}{r_0} + \frac{m^2}{r_0^2}\left(\frac{15\pi}{4} - 8\right) + \frac{2m^2}{r_0^2}\left[2\sqrt{1+R_{sm}^2} - \frac{\pi}{8}R_{sm}^2\right] + \mathcal{O}\left(\frac{m^3}{r_0^3}\right), \tag{10}$$

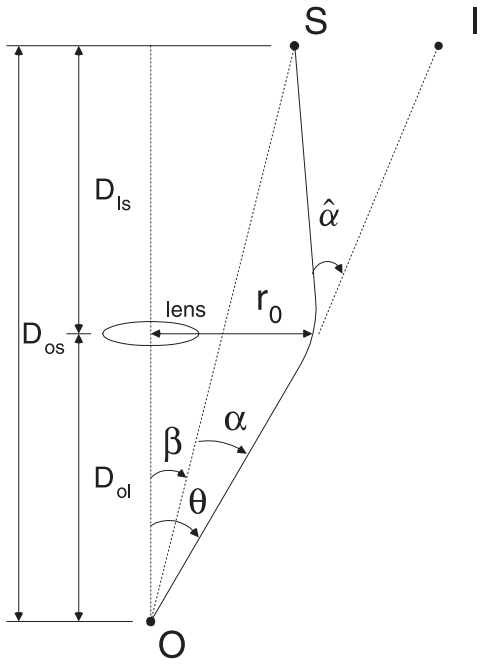

Figure 1. A typical gravitational lens diagram.

where we have written as before $R_{sm} \equiv q/m = \sqrt{1/\gamma^2 - 1}$. From this, the authors find interesting departures from GR for certain values of R_{sm}, which will also be present for the metric (3) as we shall show in the following section.

4. Image formation

The geometry for a typical GL system is shown in figure 1. A light ray coming from a source at S is deflected by an angle $\hat{\alpha}$, reaching afterwards an observer at O. The optical axis is defined as the line joining the observer and the lens; the angles between this axis and the true source position and the image position are β and θ, respectively. Hereafter, θ is the angle of the image position and is no longer one of the metric coordinates employed in the previous sections, which was set to $\pi/2$ in the null geodesic equations. The distances between observer and lens, lens and source, and observer and source are, respectively, D_{ol}, D_{ls} and D_{os}. It is customary to use, instead of $\hat{\alpha}$, the reduced deflection angle α, defined by the relation [16]:

$$\alpha = \frac{D_{ls}}{D_{os}}\hat{\alpha}.$$

From the figure, the condition for the light ray to reach the observer can be written as $\beta D_s = \theta D_s - \hat{\alpha} D_{\mathrm{ds}}$, and we have the simple expression

$$\alpha(\theta) = \theta - \beta = \frac{D_{ls}}{D_{os}}\left[\frac{4m}{D_{ol}\theta} + \frac{m^2}{D_{ol}^2\theta^2}\left(\frac{15}{4} - 4 - \frac{\pi R_{sm}^2}{4}\right)\right] + \cdots \tag{11}$$

which is called the lens equation and is in general a nonlinear equation in θ because of the dependence of $\hat{\alpha}$ on θ; this leads to the possibility of multiple images for a single source. It

should be noted that equation (11) assumes that the usual Euclidean relationship between the angle enclosed by two lines and their separation holds, namely

$$\text{separation} = \text{angle} \times \text{distance}. \tag{12}$$

However, it is not obvious that such a relation is valid in curved spacetimes, and equation (12) is actually taken as the operational definition of the so-called angular-diameter distances. Also from the diagram, we can write $r_0 = D_{ol}\theta$ for small θ. Finally, the magnification μ is defined as the ratio between the solid angles of the image and the source:

$$\mu = \frac{\theta}{\beta}\frac{\mathrm{d}\theta}{\mathrm{d}\beta} \equiv \mu_r \mu_t,$$

where

$$\mu_t = \left(\frac{\beta}{\theta}\right)^{-1} \qquad \text{and} \qquad \mu_r = \left(\frac{\mathrm{d}\beta}{\mathrm{d}\theta}\right)^{-1}$$

are the tangential and radial magnifications, respectively.

Putting all of the above together, we can now express the reduced deflection angle α as a function of the image position θ and solve the lens equation (11) for θ, thus finding the position of the images formed due to GL in the spacetime we study. We show in figure 2 the behaviour of α as a function of θ for the axially symmetric solution (full curve) as well as for the spherical one (chain curve), taking $D_{ol} = 10^9$ m, $D_{ls}/D_{os} = \frac{1}{2}$, and four different values of the ratio R_{sm}; the Schwarzschild lens is also depicted for comparison (dotted curve), and only the half-plane $\theta > 0$ is shown since the plots for $\alpha(\theta)$ are odd functions of θ.

For a given source at a position β, the image positions are found by the intersections of the straight lines $I_-(\theta) = \theta + \beta$ and $I_+(\theta) = \theta - \beta$ with the curve $\alpha(\theta)$, while the line $I_0(\theta) = \theta$ (i.e. with $\beta = 0$) represents the source aligned with the lens and the observer and the intersections with $\alpha(\theta)$ give the position of the concentric Einstein rings. Note that the value $D_{ol} = 10^9$ m is chosen so that if we take $m \sim 10^{16}$ cm, which is of the order of the mass of the Milky Way, we obtain $D_{ol} \sim 10$ Mpc, so that the results obtained can be applied to lensing by galaxies in the nearest clusters.

As was the case for the spherical lens with a scalar field, here we also observe that the contribution from the scalar field produces a maximum in α, which in turn implies the presence of additional images with respect to the Schwarzschild lens; for a fixed value of R_{sm}, there will be up to four images if β is small enough, two on each side of the source, and as β increases, the two images on the opposite side of the source come closer and eventually meet very near the position of the maximum in α, leaving three images; if β increases further, only two images are formed, both on the same side of the source; in any case, the additional images are very near the source (a few milliarcseconds), which would make them very difficult to observe. On the other hand, although the qualitative behaviour of both lenses with the scalar field is similar, as the ratio R_{sm} decreases there appear quantitative differences, as can also be seen in figure 2; however, the largest discrepancies occur for very small values of the image position, e.g. only a few milliarcseconds for $R_{sm} = 15$. Here again, the behaviour of α is identical to the Schwarzschild case for $R_{sm} < 2$, while for $R_{sm} \sim 250$ the maximum in α is so small that the images on the opposite side of the source disappear, the formation of one ring being nonetheless still possible; for even larger values of R_{sm} ($R_{sm} > 500$) two images may appear on the same side of the source, but no rings can be formed. As in GR, all the images lie on a line, since the geodesics are contained in the same plane. Table 1 shows some selected values of the positions of the images for the cases plotted in figure 2.

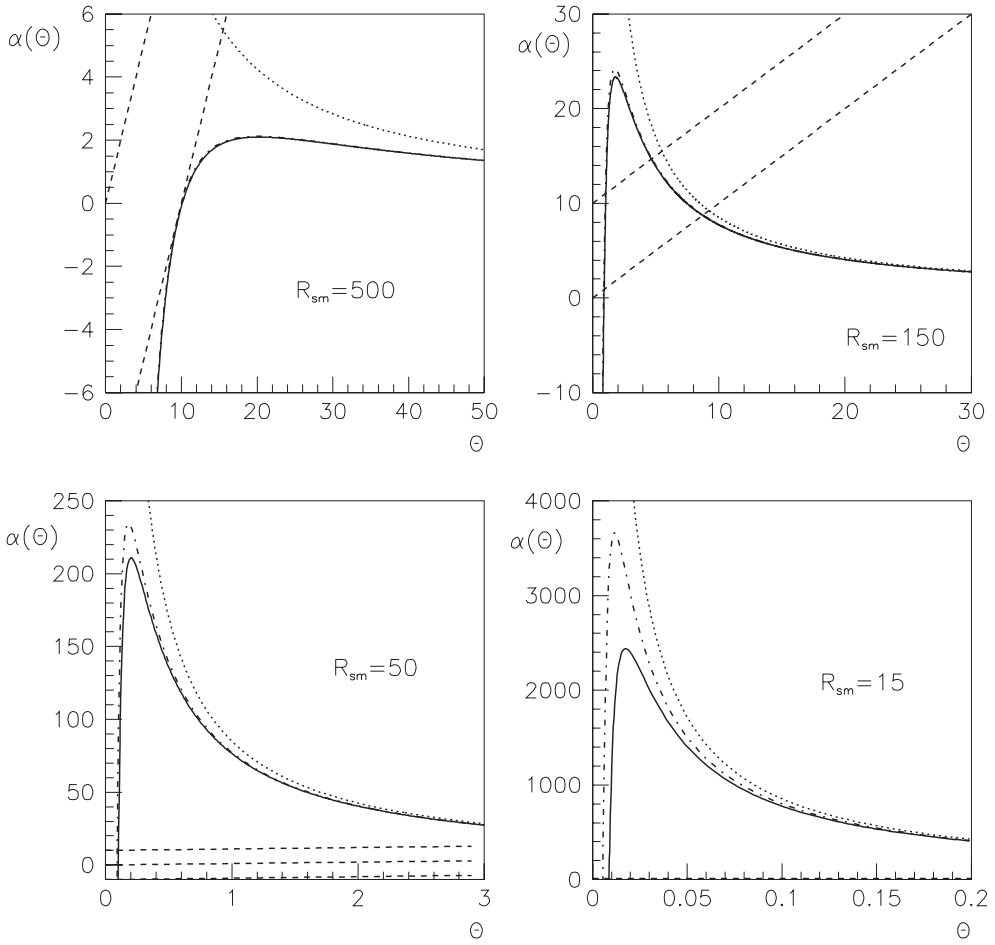

Figure 2. Reduced deflection angle α as a function of image position θ. The plot shows the axial (full curve), and the spherical (chain curve) lenses with scalar field, as well as the Schwarzschild lens (dotted curve). Also shown are the lines $I_-(\theta) = \theta + \beta$, $I_+(\theta) = \theta - \beta$ and $I_0(\theta) = \theta$. We used $D_{ol} = 10^9$ m, $D_{ls}/D_{os} = \frac{1}{2}$, and the indicated values of R_{sm}; all angles are in arcseconds.

To make another comparison, we computed the position of the maximum in the curve for α, Θ_{RCC}, which results from finding the solution to the equation $\mathrm{d}\alpha/\mathrm{d}\theta = 0$. This value is important because it indicates the position of the radial critical curve (RCC), which is a region where large radial magnifications are possible and is absent for the Schwarzschild lens. Figure 3 shows the position of the RCC for values of R_{sm} in the range from 15 to 200, as well as the fractional difference between the axial and the spherical lenses, i.e. the quantity

$$\varepsilon_\Theta \equiv \frac{(\Theta_{RCC})_{axial} - (\Theta_{RCC})_{JWN}}{(\Theta_{RCC})_{JWN}}. \tag{13}$$

It can be seen that the difference is larger for small values of R_{sm}, but unfortunately the position of the RCC is very near the lens, and as can be observed in the fourth panel of figure 2, it appears at a few milliarcseconds for $R_{sm} = 15$; at the same time, this difference tends to zero as R_{sm} grows. This indicates that, although a configuration with three or four aligned images would be a very convincing signature of an object possessing a scalar field, it might

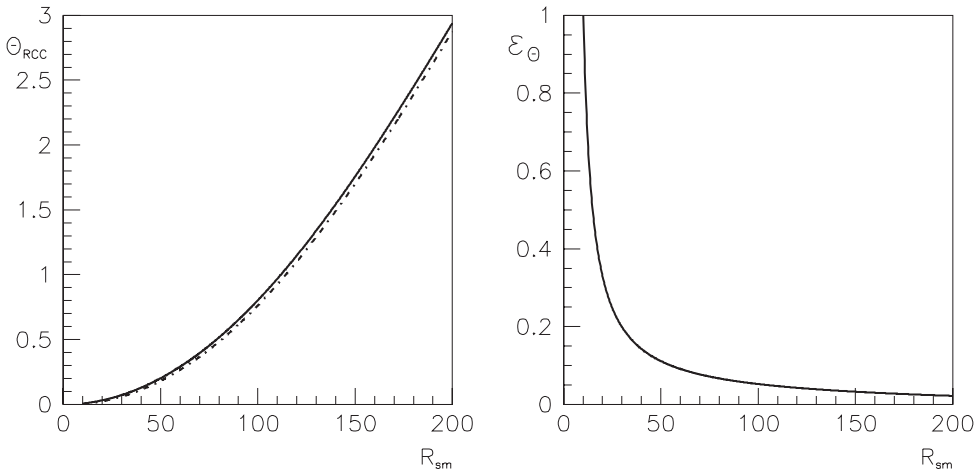

Figure 3. Position of the radial critical curve, Θ_{RCC}, for $10 < R_{sm} < 200$. The first plot shows Θ_{RCC} itself for both the axial (full) and the spherical (chain) lenses, while the second plot depicts the fractional difference ε_Θ between both cases, equation (13).

Table 1. Image positions for the axially symmetric (AS) and JNW metrics, for different values of R_{sm} and $D_{ol} = 10^9$ m, $D_{ls}/D_{os} = \frac{1}{2}$. I_+ and I_- are the images on the same and opposite sides of the source, respectively, while the superscripts o and i denote the outer and inner images. All angles are in arcseconds.

		Image position θ					
		$R_{sm} = 500$		$R_{sm} = 150$		$R_{sm} = 50$	
β	Image	AS	JNW	AS	JNW	AS	JNW
	I_+^o	—	—	11.70	11.71	12.02	12.02
5	I_+^i	—	—	0.87	0.81	0.10	0.08
	I_-^i	—	—	0.98	0.91	0.10	0.08
	I_-^o	—	—	6.40	6.41	6.99	6.99
	I_+^o	—	10.30	15.25	15.25	15.47	15.47
10	I_+^i	—	8.80	0.84	0.78	0.10	0.08
	I_-^i	—	—	1.06	0.98	0.10	0.08
	I_-^o	—	—	4.67	4.68	5.42	5.42
	I_+^o	17.03	17.06	19.22	19.22	0.10	0.08
15	I_+^i	6.17	5.99	0.80	0.75	19.37	19.37
	I_-^i	—	—	1.17	1.08	0.10	0.08
	I_-^o	—	—	3.38	3.41	4.31	4.30

not be possible to distinguish between different types of spacetimes endowed with such a field. Moreover, an independent measurement of the mass of the lens would be necessary in order to, at least, place a limit for the scalar charge of this kind of lens.

We have obtained similar results to those obtained by Virbhadra because we have studied equatorial lensing. However, off-equatorial lensing may turn out to be significantly different. In addition, our study has been done in the weak-field limit. Recently, an extensive study of Schwarzschild strong gravitational lensing has been performed by Virbhadra and Ellis [17]. They showed that due to significant bending of light at $r = 3M$, a sequences of images

on both sides of the optical axis are formed. These images are called 'relativistic images', and if they are ever observed (giving an upper bound for the closest distance of approach $r_0 = 3.21M$) that would support the black hole interpretation of the lensing object. A comparison with their results would require a strong scalar field lensing study that will be reported elsewhere.

5. Conclusions

Although an important part of different fundamental theories and of numerous alternatives or extensions to GR, the scalar field remains a hypothetical object. As part of these alternatives, it contributes to the curvature of spacetime, and therefore it should produce some macroscopic effect. As has been discussed in previous works in the literature, the use of GL seems to be a very powerful tool for trying to observe such an effect in an astrophysical setting.

In this work we have employed an axially symmetric solution to the field equations for a scalar field minimally coupled to gravity. As was discussed previously in Virbhadra *et al* [2], the presence of an object endowed with a scalar field acting as a gravitational lens would manifest through new lensing configurations. As mentioned in the introduction, it has been proposed that dark matter could be of scalar field origin. This study provides a method for deciding whether a compact object is made out of such scalar fields (for instance pulsars that have absorbed such dark matter). For values of the ratio of the scalar charge to the mass of the lens $R_{sm} \geqslant 2$, a lens of this type may exhibit three or four images, depending on the position of the source, and in particular, for a source along the optical axis ($\beta = 0$), two Einstein rings may be present; furthermore, there is a radial critical curve formed on the opposite side of the source. As R_{sm} grows, the position of the RCC moves away from the lens but at the same time the maximum in the reduced deflection angle α decreases, and for large enough values of R_{sm} (~ 250) there are no images on the opposite side of the lens. On the other hand, even though the fractional difference ε_Θ between the axial and the spherical metrics, equation (13), is very large for small values of R_{sm} ($\sim$10), the position of the RCC is very near the lens, e.g. a few milliarcseconds for the configuration considered here; finally, in spite of the RCC appearing further away from the lens as R_{sm} increases, the same difference decreases very rapidly and it tends to zero for large R_{sm}.

The above considerations allow us to say that, even if one of the configurations discussed above is ever observed, it seems to be quite difficult to distinguish between the two kinds of spacetimes with scalar field compared here; besides, one would need an independent determination of the mass of the lens in order to set a bound for the scalar charge. Finally, for values of $R_{sm} < 2$, the behaviour of both lenses is the same as the Schwarzschild lens: there is no RCC and there is one image on either side of the lens; this is to be expected, since a small ratio R_{sm} means a scalar field which is weak compared with the mass of the lens.

Acknowledgments

This work was partly supported by CONACyT, México, under grants 3697-E (TM) and 32885-E (RB).

References

[1] Damour T and Esposito-Farèse G 1993 *Phys. Rev. Lett.* **70** 2220
[2] Virbhadra K S and Narasimha D, Chitre S M 1998 *Astron. Astrophys.* **337** 1
[3] Guzman F S, Matos T and Villegas H 1999 *Astron. Nachr.* **320** 97

[4] Cho Y M and Keum Y Y 1998 *Class. Quantum Grav.* **15** 907
[5] Matos T and Ureña-López L A 2000 *Phys. Rev.* D **62** 081302(R)
Matos T and Ureña-López L A 2000 *Class. Quantum Grav.* **17** L75–81
Matos T and Ureña-López L A 2001 *Phys. Rev.* D **63** 063506
[6] Kolb E and Turner M 1993 *The Early Universe (Addison-Wesley Advance Book Series no 123)* (Reading, MA: Addison-Wesley)
[7] Wyman M 1981 *Phys. Rev.* D **24** 839
[8] Virbhadra K S 1997 *Int. J. Mod. Phys.* A **12** 4831
[9] Janis A I, Newman E T and Winicour J 1968 *Phys. Rev. Lett.* **20** 878
[10] Matos T 1998 *Gen. Rel. Grav.* **30** 5
[11] Matos T, Núñez D and Quevedo H 1995 *Phys. Rev.* D **51** R310
[12] Matos T 1998 *Phys. Lett.* A **249** 271
[13] Matos T and Becerri R, in preparation
[14] Chandrasekhar R 1983 *The Mathematical Theory of Black Holes* (Oxford: Oxford University Press)
[15] Weinberg S 1972 *Gravitation and Cosmology* (New York: Wiley)
[16] Narayan R and Bartelmann M 1998 Lectures on gravitational lensing *Formation of Structures in the Universe: Proc. 1995 Jerusalem Winter School* ed A Dekel and J P Ostriker (Cambridge: Cambridge University Press) (Narayan R and Bartelmann M 1996 *Preprint* astro-ph/9606001)
[17] Virbhadra K S and Ellis G F 2000 *Phys. Rev.* D **62** 084003
[18] Garfinkle D, Horowitz G T and Strominger A 1991 *Phys. Rev.* D **43** 3140